

Study of the feasibility of the MASW seismic method in coal prospecting: a study based on a conceptual model for the Candiota mine, southern Brazil

<http://dx.doi.org/10.1590/0370-44672023770141>

Lucas Rosso Lopes^{1,3}

<https://orcid.org/0000-0003-0667-9328>

Marcus Vinicius Aparecido Gomes de Lima^{1,4}

<https://orcid.org/0000-0001-5912-1032>

Randell Alexander Stephenson^{2,5}

<https://orcid.org/0000-0003-4868-8601>

¹Universidade Federal do Pampa – UNIPAMPA, Campus Caçapava do Sul, Caçapava do Sul – Rio Grande do Sul - Brasil.

²University of Aberdeen, School of Geosciences, Aberdeen - United Kingdom.

E-mails : ³rosso_geo96@gmail.com,

⁴marcuslima@unipampa.edu.br,

⁵r.stephenson@abdn.ac.uk

Abstract

The main coal reserves in Brazil are located in the southern region, where the most important coalfield, including the Candiota mine, is found. The mineral exploration and mine planning programs of the companies mining these coal deposits are generally restricted to drilling data and cores, despite the exploratory potential of geophysical methods in coal prospecting. This study aims to investigate the ability of the seismic method known as Multichannel Analysis of Surface Waves (MASW) to identify coal seams in the Candiota area. The MASW method allows obtaining a layer model composed of a low-velocity (blind) layer and/or relatively thin (hidden) layer from the surface wave dispersion curves. The hidden and blind layer problems are pitfalls of the traditional seismic refraction method and the geological settings related to coal seams may encompass both problems. In addition, the Candiota mine has conditions favorable for applying the MASW method due to the shallow depths of the coal seams. The study was based on the analysis of synthetic seismic data generated from a 3-layer conceptual model of the Candiota deposit. The dispersion curves of the fundamental mode of the Rayleigh surface waves were generated and the effects of each of the parameters of the seismic model were evaluated, as well as the relationship between the parameters through objective function tests. A new inversion algorithm capable of obtaining the true model was implemented. The results obtained from the application of the inversion algorithm demonstrated the potential of the MASW method in identifying coal seams from S-wave profiles and proves it to be a powerful tool for coal mineral exploration programs.

Keywords: mineral exploration; coal prospecting; seismic method; Multichannel Analysis of Surface Waves; Candiota deposit.

1. Introduction

Coal is an abundant fossil fuel, with reserves widely located around the world. Despite recent policies to accelerate a transition to cleaner energy sources, the growing demand for energy sources leaves coal as an important and strategic natural resource, particularly in emerging countries, ensuring price stability. Currently, coal is responsible for about 27% of the world's primary energy consumption (Thomas,

2023). Part of the coal produced is destined for the metallurgical industry, being used in the production of 71% of the global steel (World Coal Association, 2009).

In Brazil, coal is mainly used by thermal power stations to complement the energy matrix (CRM, 2018). Coal deposits are located in southern Brazil. The Brazilian Electricity Regulatory Agency (in Portuguese, Agência Nacional

de Energia Elétrica, ANEEL) estimates that the state of Rio Grande do Sul has 88% of the reserves, of which 38% of national coal production is provided by the Candiota mine.

Mineral prospecting and coal mining planning is traditionally carried out using models created based on geological drilling and field surveys that are relatively expensive and provide discrete informa-

tion, as opposed to continuous results of geophysical profiles. Integration with geophysical data allows a more reliable modeling of the subsurface coal deposits (Krey, 1963; Buchanan, *et al.*, 1981; Gochioco & Cotten, 1989; Gochioco, 1990; Gochioco, 2000). The geophysical data commonly used for coal prospecting consist of well-logging, used to identify the layer, and estimate the quality of coal (Hatherly, 2013), such as electroresistivity logs, natural gamma and density (gamma-gamma) (Christoffel & Kayal, 1989; Webber *et al.*, 2009; Souza *et al.*, 2010).

The contrast of physical properties of coal with the host rock also enables the use of geophysical methods in the lithological characterization of these subsurface layers. For example, carbonaceous sequences are generally characterized by low values of seismic velocity and density in relation to other sedimentary rocks (Dresden & Ruter, 1996). As a result, seismic methods have been widely applied in coal exploration since the 1960s (Krey, 1963; Costa *et al.*, 1978; Bentes & Costa, 1979; Costa & Dias, 1982; Gochioco

& Cotten, 1989). For instance, high-resolution reflection seismic imaging has been shown to be efficient in mapping coal seams and identifying geological faults (Greenhalgh *et al.*, 1986).

In this study, because of the shallow depth of the coal seam (< 50 m) of the Candiota deposit, using surface waves in seismic data provides favorable conditions and possibilities for mineral prospecting. Herein, a study of the application of the seismic method known as Multichannel Analysis of Surface Waves (MASW) to obtain representative S-wave models of coal seams is presented. First, the use of the method based on the sensitivity analysis of the seismic parameters (V_p , V_s , density) and thickness of the layer model is investigated. The tests are performed considering synthetic data generated from models built based on information obtained from drillholes at the Candiota mine.

The MASW method allows resolving models with a low velocity layer (hidden layer), which is one of the limitations of the application of the seismic

refraction method. Furthermore, the method provides S-wave models from data generated from predominantly compressive seismic sources recorded by vertical sensors only. For this reason, MASW is one of the most suitable surface geophysical tools for coal prospecting and the inversion approach employed is effective in terms of sensitivity and relationship between the physical properties of the subsoil.

In order to solve the non-uniqueness problems inherent to geophysical inversion and overcome some limitations of the available software (such as Dinver, SWAN, etc.), mainly with regard to the determination of the thickness of the low velocity layers, as in the case of coal sequences, we have implemented the Controlled Random Search algorithm (CRS). The code was written in Python language incorporating Geopsy modeling tools (gpdc). CRS is a global optimization algorithm that searches through random models exploring more widely the solution space, avoiding local minima of the objective function (Price, 1977).

2. Geological setting of the study area

The study area is located in Candiota, state of Rio Grande do Sul, southern Brazil (Figure 1).

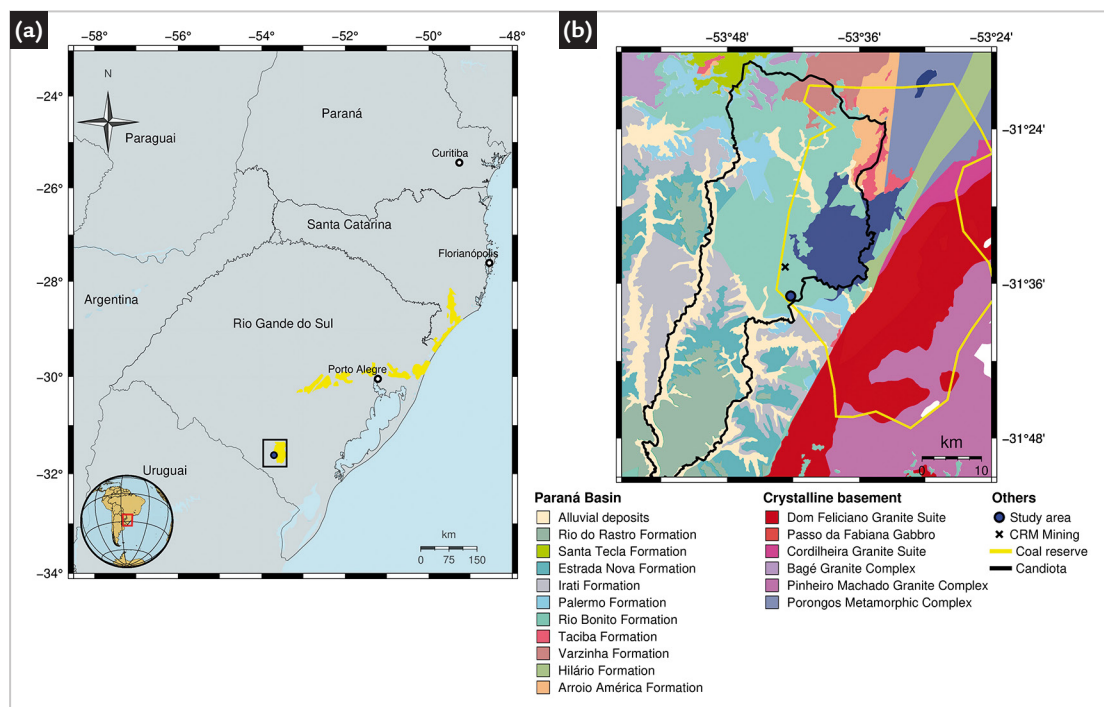


Figure 1 - (a) Map of southern Brazil and neighboring countries highlighting the locations of the mineral coal deposits (yellow features). Geographical boundaries are indicated by plain black lines and capitals represented by white circles. Reference cities, states and countries are properly labeled on the map. The area depicted by the black rectangular outline points to the location of the Candiota Coalfield. The inset map shows the southern Brazil in the context of the South American continent; and (b) geological setting map of the Candiota mine showing the formations of the Paraná Basin (Paleozoic to Recent sedimentary and volcanic strata) and basement (Precambrian crystalline igneous and metamorphic rocks). The boundary of the municipality of Candiota and the coal reserve are represented by polygons with plain black and yellow contours, respectively.

According to Silva (1993), the coal seams in Candiota are attributed to the Rio Bonito Formation (290.6 ± 2.8 Ma and 281.7 ± 3.2 Ma; Cagliari *et al.*, 2014) of the Paraná Basin. The coal deposits of the Rio Bonito Formation have been studied since the 19th century, and Machado & Castanho (1956) used the term Rio Bonito Formation to describe the fluvial-lacustrine continental sediments, with intercalations of carbonaceous beds between the Itararé Group and the Palermo (Holz & Kalkreuth, 2004).

The stratigraphic sequence analysis described by Holz *et al.* (2000) establishes that the coal seams of economic potential of the Rio Bonito Formation are associated with a lagoon-barrier depositional system. The Rio Bonito Formation is initially marked by a low-sea system tract followed by a trans-

gressive system tract, in which the most important coal seams were deposited. The transgressive system tract can be divided into four parasequences: the first is composed of sandstones that are onlap on the low sea system tract; the second is formed by storm beds from a barrier-lagoon island system where the coals form the lower layers; the third parasequence is composed of stormflood cycles that formed the coal layers; and in the fourth parasequence, the deposition of peat was not sufficient for the formation of coal (Holz & Kalkreuth, 2004).

The Candiota coalfield corresponds to a sequence of thin coal layers interbedded with sandstones, claystones and shales. The average thickness of the coal seam package is 4.5 m, in places reaching 6 m (Gomes *et al.*, 1998). Silva & Kalkreuth (2005) classified Candiota

coal as sub-bituminous (low rank A) according to the international classification (UN-ECE). Currently, the Candiota deposit is being mined by Companhia Riograndense de Mineração (CRM) and Seival Sul Mineração (SSM).

Figure 2 shows the lithostratigraphy of the MVI-39 well in the CRM area. At the location of this borehole, the Candiota deposit corresponds to three layers of coal a few meters thick: Banco Louco corresponds to a layer less than 1 m thick, being the shallowest coal layer, followed by the Banco Superior and Banco Inferior layers, each exceeding 2.5 m thickness located at about 20 m deep in the study area, intercalated between thin packages of waste rock. The roof strata of the mined coal seam is composed of sandstone, claystone and shale. The floor stratum is predominantly composed of sandstone.

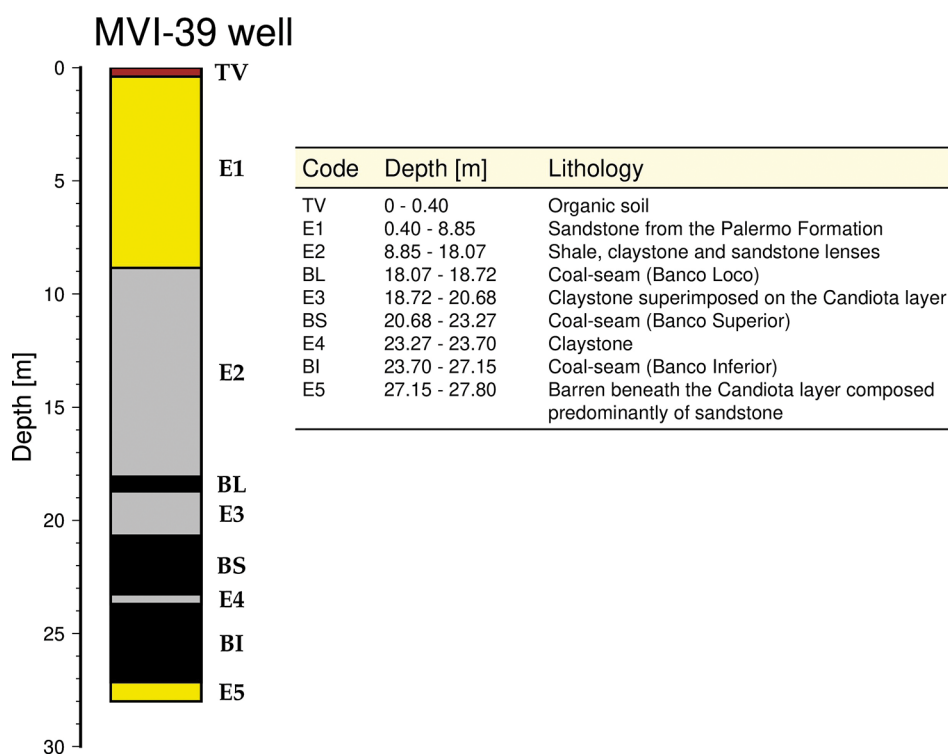


Figure 2 - Lithological description of the MVI-39 well.

3. MASW method

Seismic methods are based on the propagation of elastic waves through the Earth (Lowrie, 2007). Surface waves are the part of the seismic wavefield that travel along or near the surface of the ground, the wave motion falling off rapidly with depth. It is characterized by relatively low velocity, low frequency, and high amplitude. In seismic exploration, it is usually referred to as ground roll and mainly comprises what are known as Rayleigh waves. The presence of near-surface stratigraphic layers, such as seen in Figure 2, causes surface

wave dispersion, which is the variation of velocity with frequency. The phenomenon of dispersion is observed from the change in waveform with the separation of surface waves due to the propagation of different wavelengths through different depth ranges, and hence, different phase velocities (Sheriff & Geldart, 1995).

The Multi-channel Analysis of Surface Waves (MASW) method, introduced by Park *et al.* (1999; 2007), uses the dispersion curve from the spectral analysis of surface waves to infer an S-wave velocity

profile, indicating subsurface lithological and/or petrophysical changes, which can be obtained by ground-roll analysis. This method allows identifying layers that could not be imaged by the high-resolution seismic reflection method, due to the intrinsic resolution limit. The analysis of MASW involves three steps: acquisition of the ground-roll, construction of dispersion curves of the fundamental and harmonic modes in terms of phase velocity by frequency, and inversion of these curves to obtain 1D structure models of S-wave velocity (Foti *et al.*, 2018).

4. CRS inversion algorithm

A number of inversion algorithms have been formulated to obtain robust models in multidimensional parameter space (Olsson & Nelson, 1975; Price, 1977) and various geophysical data inver-

sion software packages have been developed from these algorithms. The present study uses the Controlled Random Search (CRS) inversion algorithm to search for global minima of multimodal functions.

The CRS algorithm is versatile and can be adapted to any kind of multi-dimensional global optimization problem, constrained or unconstrained. The main aspects of the CRS workflow are presented in Figure 3.

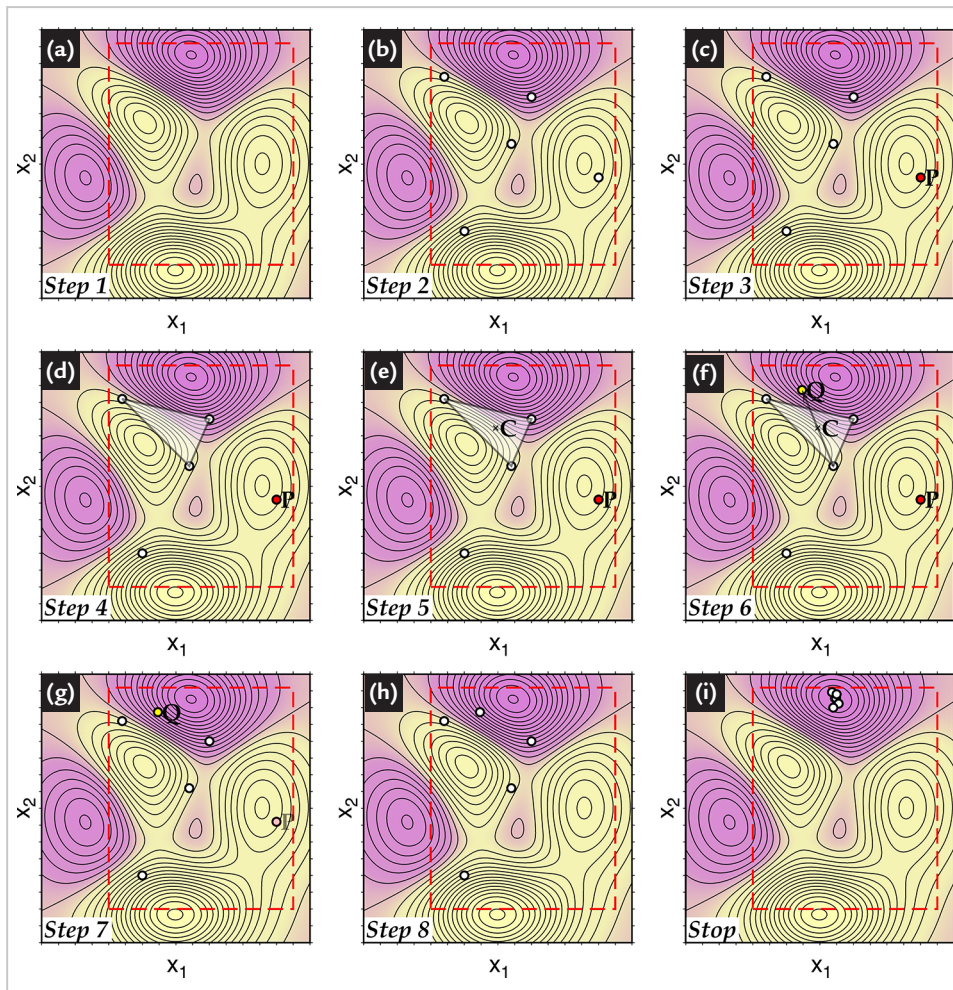


Figure 3 - Schematic diagram illustrating the CRS algorithm search procedure for an arbitrary

two-dimensional objective function, $f_{obj}(x_1, x_2)$, where x_1 and x_2 are model parameters ($n = 2$). In this example, a set of

five points ($N = 5$ models) delimited by the search domain V (dashed red rectangle) is used: Step 1 – Set the search domain, V ;

Step 2 – Randomly choose N points; Step 3 – Determine the highest f_{obj} point; Step 4 – Randomly choose $n+1$ points to form a simplex;

Step 5 – Calculate the centroid C of the simplex; Step 6 – Determine the new point Q from the centroid; Step 7 – Replace P with Q if $f_{obj}(Q) < f_{obj}(P)$; Step 8 – Repeat steps 2 to 7 until the stopping criterion is satisfied; and Stop – Points converged to the minimum of the f_{obj} .

Some examples of the application of CRS in geophysical inversion are found in Silva & Hohmann (1983), Smith *et al.* (2000), Bortolozzo *et al.* (2015) and Di Maio *et al.* (2016). Furthermore, modified and improved versions of the algorithm are described by Křivý & Tvrdík (1995), Kaelo & Ali (2006) and Charilogis *et al.* (2021).

First, the user defines the search

range of a domain V for each of the n parameters of the model and the N random search points in the parameter space (steps 1 and 2). The parameter space is a multi-dimensional space where each dimension corresponds to one parameter and each point represents one model. The value of the objective function is calculated for each random point and stored in vector A , for

which the point P with the highest value of the objective function $f_{obj}(P)$ is determined (step 3). At each iteration of the algorithm, $n+1$ points are chosen randomly for the construction of a “simplex”, where a new point Q will be determined from the reflection of the $(n+1)$ th point (H) with respect to the simplex centroid (C) (steps 4-6) given by the following equation:

$$Q = 2 \cdot C - H \quad (1)$$

If point Q is contained in domain V , its objective function $f_{obj}(Q)$ is calculated. If $f_{obj}(Q)$ is less than $f_{obj}(P)$,

P is replaced by Q in A . If $f_{obj}(Q)$ is greater than $f_{obj}(P)$, then the point Q is discarded, and a new iteration of the

algorithm is performed. Iterations are performed until the stopping criterion is satisfied.

5. Model set-up: parameter resolution and sensitivity

As coal deposits are found in sedimentary basins, their geology is characterized by the occurrence in beds, called seams, which are blanket like coal deposits a few centimeters to tens of meters thick. Despite the structural complexity of the various depositional environments, in addition to tectonic processes, such as folding, faulting and erosion, in most cases coal seams can be geologically represented by a horizontally layered medium.

Coal typically presents anomalous geophysical responses in relation to the other lithologies of a usual carbonaceous sequence given its contrasting physical properties. In general, coal is characterized by lower density, lower seismic velocity (both P and S waves),

lower radioactivity, lower magnetic susceptibility, and higher electrical resistivity than typical adjacent rocks (Dresden & Ruter, 1996). The values of seismic velocity and density of coal can vary according to its composition and quality (rank). According to Morcote *et al.* (2010), the seismic velocity of coal increases with increasing rank. However, large variations in seismic velocity of sedimentary rocks are also associated with rock depth and its age, being higher with increasing depth and deposition time.

A synthetic 3-layer seismic model was designed for the local geological setting of the Candiota mine and the reference P-wave velocity in coal seams (Kokowski *et al.*, 2019). S-wave veloci-

ties were defined from typical Poisson's ratio values (Tian *et al.*, 2019). The model consists of a 20 m thick non-coal sedimentary layer overlying a 2 m layer, representing the Banco Superior layer, both overlying a non-coal sedimentary layer.

Table 1 shows the values of the parameters and ranges of the investigated synthetic model. The model geometry is relatively simple (rock-coal-rock) in order to allow an unbiased analysis of the relationship between the seismic parameters. The parameter ranges were defined based on the minimum and maximum velocities of the admissible Poisson's ratio, and to produce a wide variety of model types for testing.

Table 1 - Synthetic 3-layer seismic model physical parameters with variation ranges described in square brackets.

Layer	Thickness - Depth (top - bottom) (m)	V _p (m/s)	V _s (m/s)	Density (kg/m ³)	Poisson's ratio
1	20 (0 - 20) [10 - 30]	1400 [1200 - 1600]	770 [570 - 970]	2100 [1900 - 2300]	0.28 [0.15 - 0.35]
2	2 (20 - 22) [1 - 3]	1200 [1000 - 1400]	600 [400 - 800]	1700 [1500 - 1900]	0.32 [0.10 - 0.44]
3	∞ - (22 -)	1400 [1200 - 1600]	770 [570 - 770]	2100 [1900 - 2300]	0.28 [0.15 - 0.35]

Resolution and sensitivity tests were performed evaluating the effect of each model parameter on the Rayleigh fundamental mode dispersion curves. From the synthetic model (Table 1), each of the parameters (V_p, V_s, density and thickness) of each layer of the model were changed individually to verify their influence on the dispersion curve (Figure 4).

For forward modeling of theoretical dispersion curves, the **gpdc** tool provided by the Geopsy package was used. The equations and methods implemented in the tool are fully detailed in the software documentation and reference links available (Wathelet *et al.*, 2020). In short, the computation of theoretical dispersion curves is based on efficient solutions of the eigenvalue problem. Gpdc, for example, has a mode search control, called mode jumping, which detects modal curves even where they might be located very close to each other at certain frequencies: at high frequency or at osculation points for the case of Rayleigh waves.

The fundamental modes of the dispersion curves were computed for

the frequency range from 1 to 100 Hz. In this frequency span, the multimodal energy of surface waves can exhibit a very complicated distribution at high frequencies. Despite this, for practical purposes of computational implementation, the effects of osculation of the fundamental and higher modes were not considered in the analysis.

In Figure 4a-c, we initially analyzed the case of the influence of V_p with the other parameters fixed at the original value. By varying V_{p1} and V_{p3} between 1200 and 1600 m/s and V_{p2} between 1000 and 1400 m/s, we showed that V_{p1} causes only small variations in the higher frequencies of the curves, while V_{p3} generates small variations in the lower frequencies. Thus, it can be considered that the V_p profile has a negligible influence on the dispersion curves; that is, the contrast of the layers in terms of V_p does not directly affect the dispersion of surface waves.

In Figure 4d-f, only the variations of V_s are represented while V_p, density and thicknesses held constant. V_{s1} and V_{s3} were changed from 570 to 970 m/s

and V_{s2} varied between 400 to 800 m/s. It was observed that the curves at low frequency are not influenced by V_s of the first layer, causing changes of the curves at high frequency. On the contrary, the effects of the V_{s3} disappeared at high frequency. The influence of V_{s2} is verified mainly in the intermediate frequencies.

The influence of the densities (ρ) is tested in Figure 4g-i and notice that this parameter does not affect the dispersion in the same way.

Finally, the influence of the thickness of layers 1 and 2 was investigated. In the first case, variations of h₁ change the depth of the second layer. Consequently, the effects at high frequencies tend to increase in the curves as the top of the second layer becomes shallower. The influence of h₂ was restricted to intermediate frequencies. Increasing the layer thickness caused an increase in the effect produced on the dispersion curve; however, the magnitude of these changes was clearly subtle. Therefore, the resolution of this parameter depends on the quality of the experimental data.

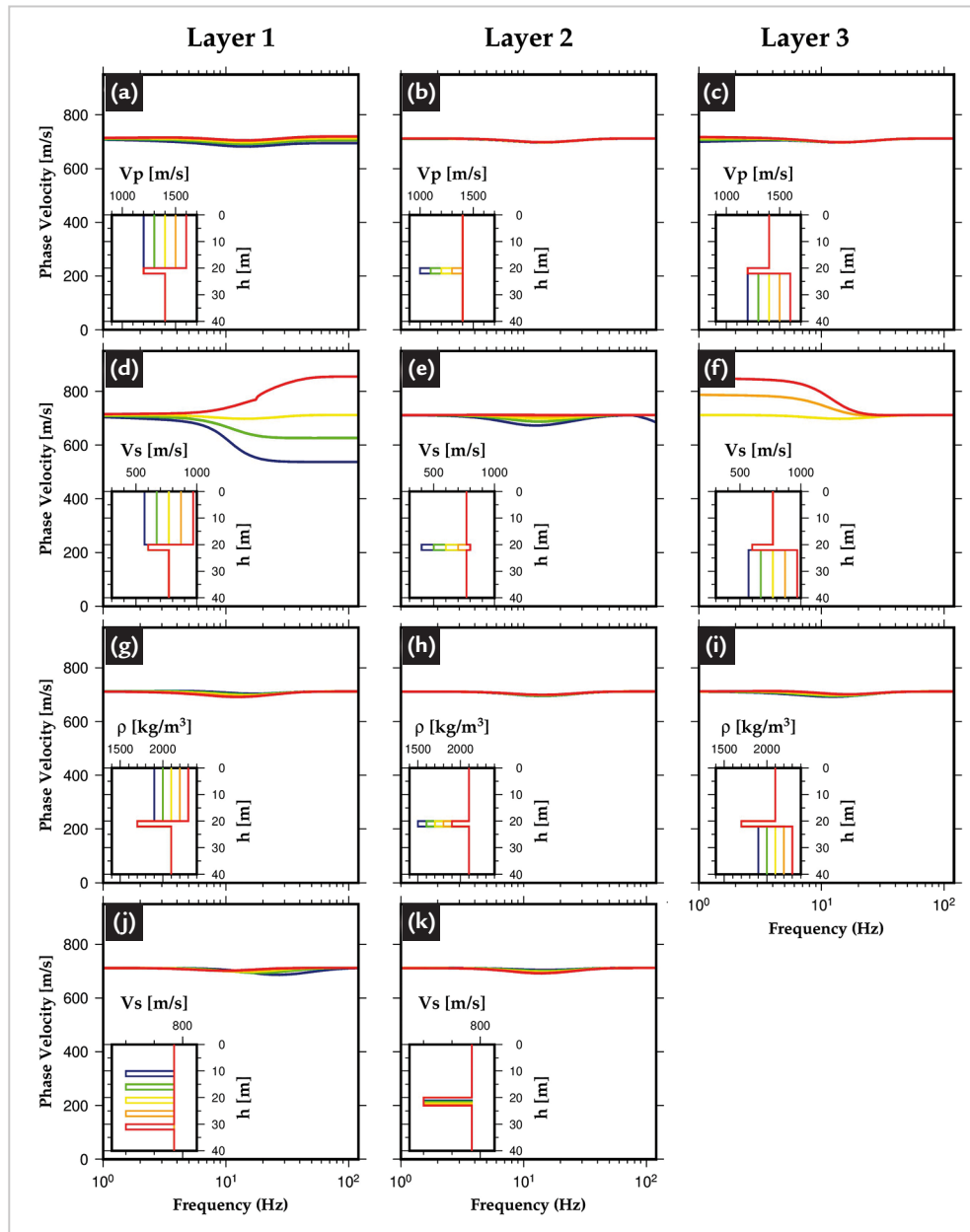


Figure 4 - Sensitivity analysis of the Rayleigh dispersion curves against layer parameters: fundamental mode dispersion curves of the Rayleigh waves in terms of phase velocity (ordinate axis) by frequency (abscissa axis) for a 3-layer seismic model individually varying V_p , V_s , density and thickness of each layer of the model (profiles shown in the inset). The models and their corresponding dispersion curves are represented by distinct colors. The subscript index the layer number.

6. Analysis of the objective function

The objective function, also known as cost, loss or misfit functional, plays a key role in optimization algorithms applied to inverse problems. The goal of the algorithm is to find the values of the parameters

that minimize or maximize the objective function. The mathematical formulation that defines the objective function, in practice, measures the misfit between the observed data value and the computed value from the for-

ward model, using a set of parameters chosen from the model space. In the present case, the calculated objective function is the L^2 -norm, also called the Euclidean norm, which is represented by Equation 2:

$$f_{obj} = \sqrt{\sum_{i=1}^{nf} \frac{(v_{di} - v_{ci})^2}{nf}} \quad (2)$$

Where f_{obj} is the misfit-value that represents the distance between the calculated dispersion curve and the observed curve, v_{di} is the observed

dispersion velocity at frequency f_i , v_{ci} is the calculated velocity at frequency f_i , and nf is the number of frequency samples considered.

The analysis of the objective function is essential for understanding the nature of the inverse problem, especially of non-linear functions. Since

the number of model parameters is 11 (V_{P1} , V_{P2} , V_{P3} , V_{S1} , V_{S2} , V_{S3} , ρ_1 , ρ_2 , ρ_3 , h_1 and h_2), the multi-dimensional visualization of parameter space would be physically unfeasible. Therefore, in order to carry out a study of the behavior of the objective function, hyperplanes (cross-sections of the parameter space) are generated by combining all possible pairs of model parameters, varying the values of two parameters and setting the other parameters to the correct values. Thus, 55 sections were generated

corresponding to each of the possible pair combinations of the 11 model parameters (Figures 5, 6 and 7). The intervals used in the hyperplanes of the objective function f_{obj} are the same used in the analysis of the dispersion curves in Figure 4.

This graphical representation allows establishing the correlation between pairs of parameters of the seismic model and inferring the degree of ambiguity and level of uncertainty of the obtained model parameters. By analogy, we can

interpret the cross-sections of the objective function as topographic maps, where the relief depicts the theoretical/predicted complexity of the inverse problem and the lowest elevation values indicate possible solutions (local and global minima). In this way, from the visual assessment of the sections, it can be observed that:

- i) there is an absence of isolated local minima within the investigated ranges;
- ii) there is a presence of a typical valley-shaped pattern in the sections of V_s (Figure 5a, b, c, e, g, h, i, l, m, n, p, w, x, y, z, a').

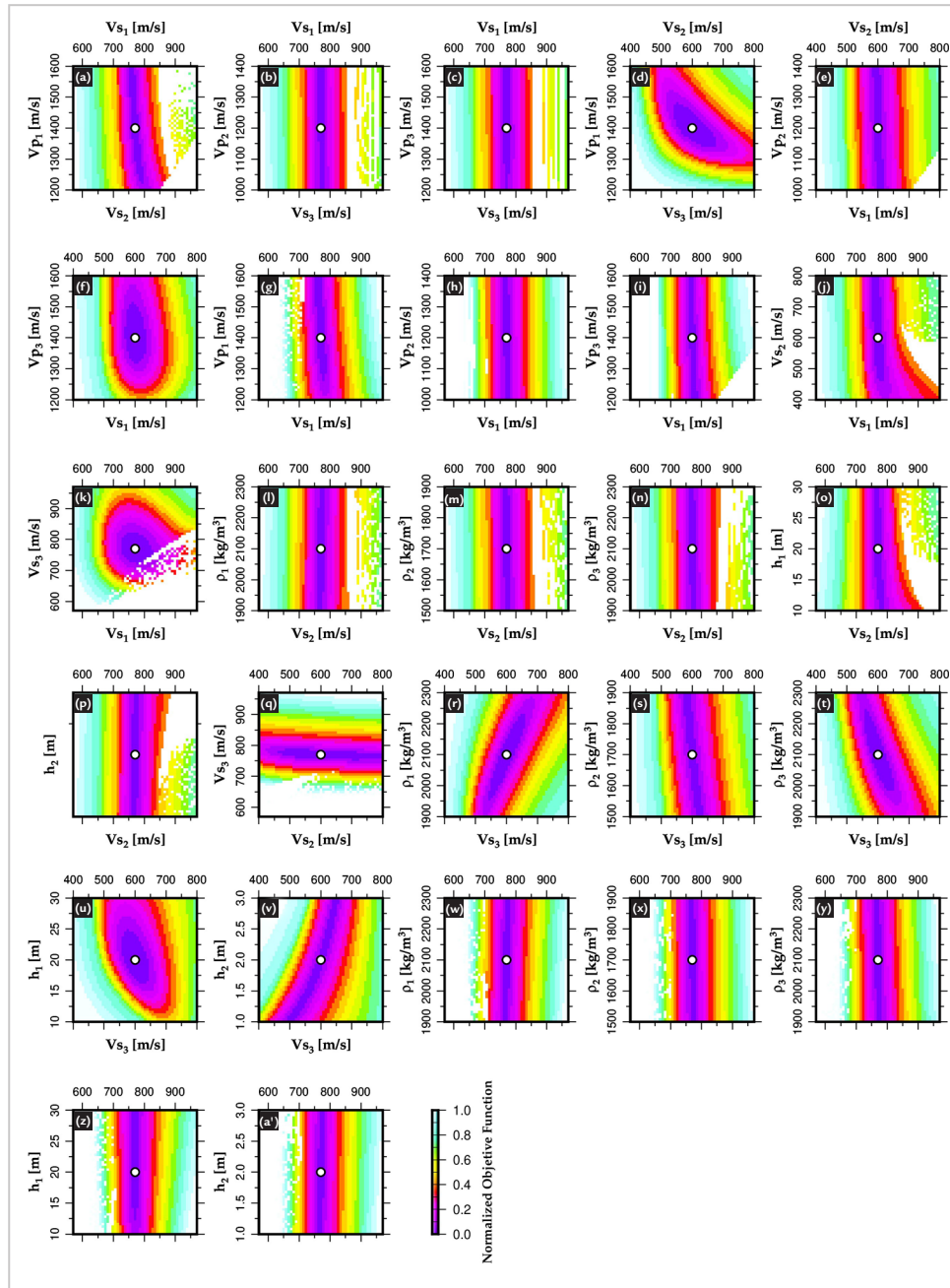


Figure 5 - Two-dimensional cross-sections (hyperplanes) of the multi-dimensional parameter space representing the surface of the objective function for a particular pair of parameters while the other parameters are fixed to their correct values: a - a') Objective function maps (similar to “topography charts”) resulting from combining the V_s of the three layers with all model parameters. True parameter values are centered in the graphs and indicated by white circles. The areas of the graphs that do not show objective function values (blank area) are due to the lack of contrast of physical properties for that combination of parameters or when the Poisson ratio converges to negative values.

This characteristic indicates that the parameter orthogonal to the valley axis, for example Vs_1 in Figure 5c, presents a unique and well-defined solution for the parameter. On the other hand, it is not possible to determine the true value of the parameter parallel to the valley, because any points along the axis result in equal objective function values;

iii) in general, hyperplanes in Figure 5 show that Vs is the best resolved parameter, particularly Vs_1 and Vs_3 . Vs_2 tends also to be resolved; however, the

convergence is highly dependent on the layer thicknesses h_1 and h_2 (Figure 5u-v);
 iv) Vp_1 , when associated with densities, thicknesses or $Vp_2 - Vp_3$, presents a behavior similar to that of Vs . Vp_2 is the highest uncertainty parameter (Figure 6h-m); that is, the variation of the values of Vp_2 in relation to the other parameters produces small variations in the objective function. Vp_3 does not show significant correlation with the other parameters (slightly elliptical circular pattern) (Figure 6n-r);
 v) apparently, the objective func-

tion depends weakly on the values of densities (Figure 5l, m, n, r, s, t, w, x, y), showing greater confidence level only in relation to Vp_2 (Figure 6i-k); and
 vi) despite the high uncertainty in the estimation of thicknesses, h_1 and h_2 have a direct influence on the determination of other parameters, mainly on Vs_2 (Figure 5u-v). In addition, observe that there is a positive correlation between h_2 and ρ_3 and a negative correlation between ρ_1 and h_2 (Figure 7i and 7d, respectively).

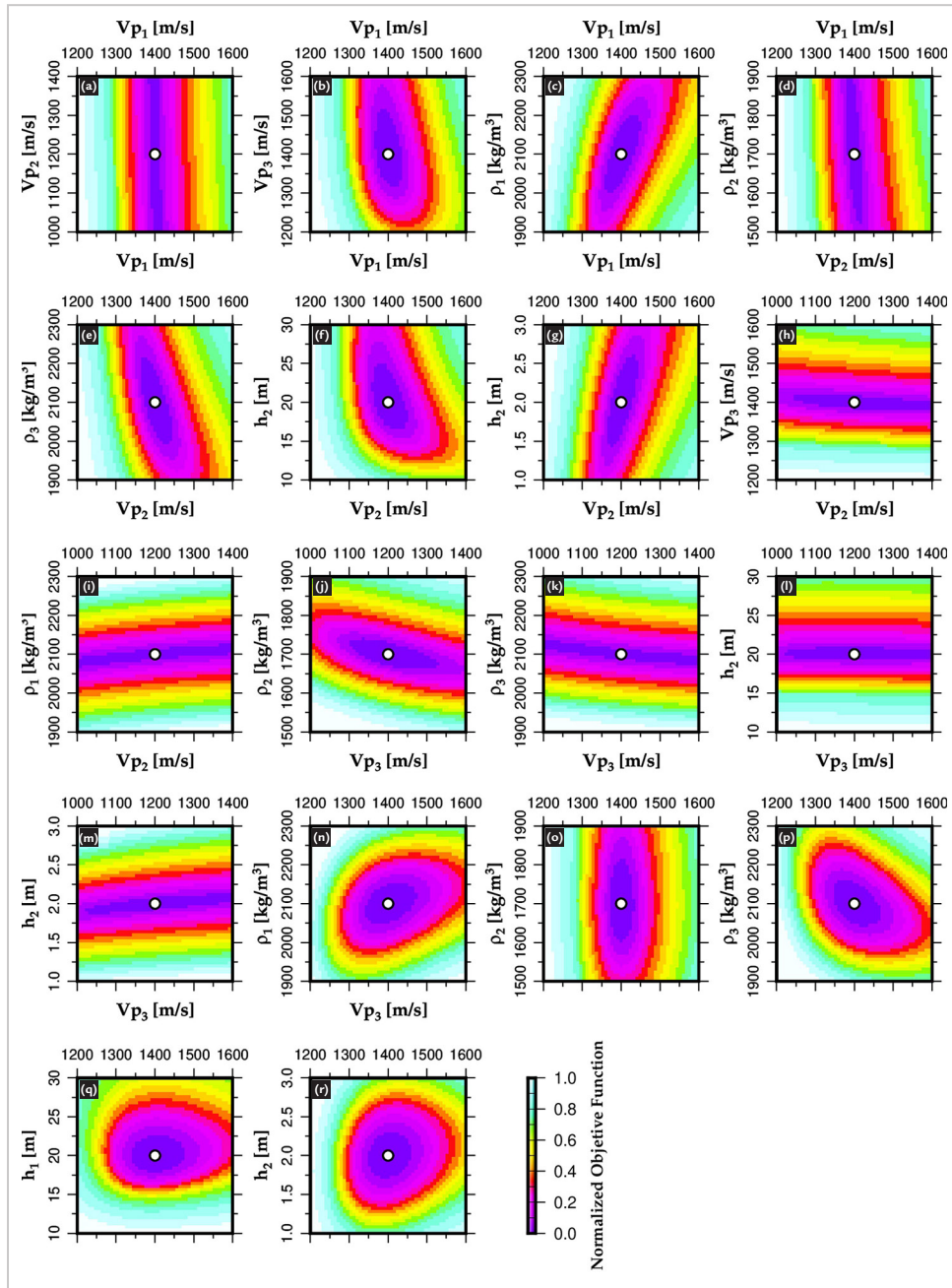


Figure 6 - Two-dimensional cross-sections (hyperplanes) of the multi-dimensional parameter space representing the surface of the objective function for a particular pair of parameters while the other parameters are fixed to their correct values: a - r) Objective function maps (similar to topographic maps) resulting from combining the Vp of the three layers with the model densities and thicknesses. True parameter values are centered in the graphs and indicated by white circles. The areas of the graphs that do not show objective function values (blank area) are due to the lack of contrast of physical properties for that combination of parameters or when the Poisson ratio converges to negative values.

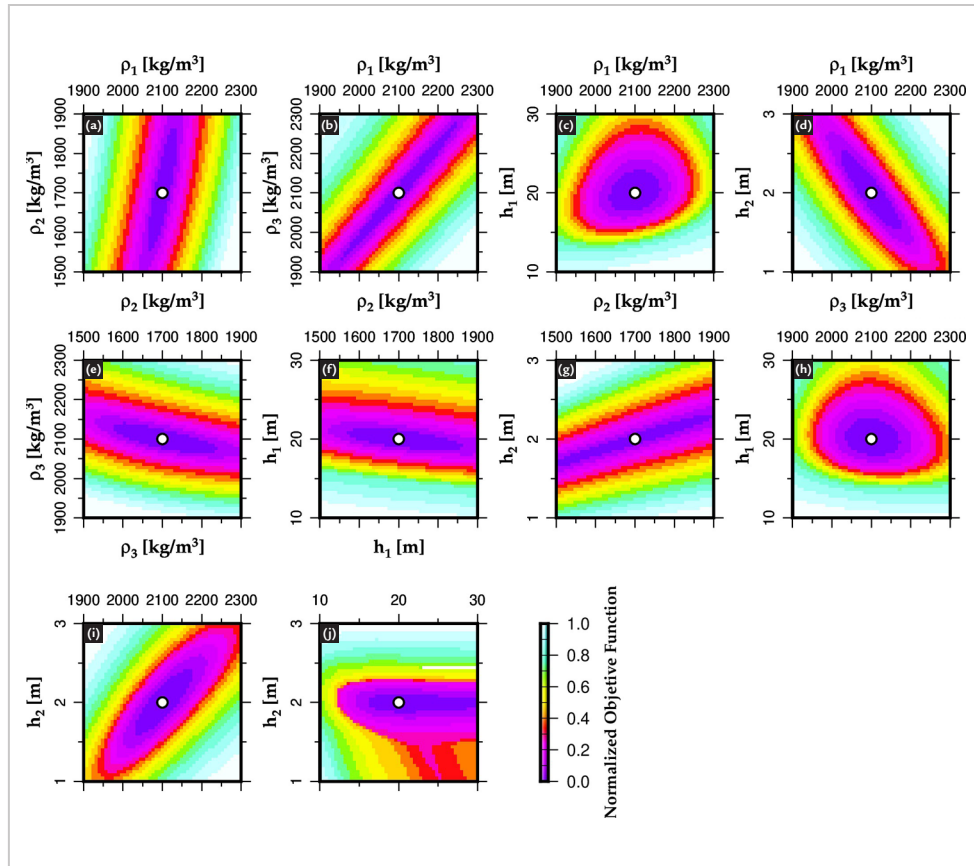


Figure 7 - Two-dimensional cross-sections (hyperplanes) of the multi-dimensional parameter space representing the surface of the objective function for a particular pair of parameters while the other parameters are fixed to their correct values: a - j) Objective function maps (similar to topographic maps) resulting from the combination of model densities and thicknesses. True parameter values are centered in the graphs and indicated by white circles. The areas of the graphs that do not show objective function values (blank area) are due to the lack of contrast of physical properties for that combination of parameters or when the Poisson ratio converges to negative values.

7. Inversion algorithm

The CRS inversion algorithm was implemented from a set of scripts written in Python version 3 in order to verify the algorithm's ability to retrieve the true velocity model corresponding to a coal seam initially defined by a dispersion curve. The gpdc tool was imported as a system module in the algorithm for the iterative calculation of dispersion curves for each model generated. To execute the algorithm, a number of model layers and a search domain are initially established for each of the $n=11$ parameters. An initial population of $N=110$ random models was created, the objective function was calculated for each of the models, and the model with the highest value of the objective function was defined. $n+1$ models were randomly chosen for the assembly of a *simplex*, and from this, a new model was obtained with the rebound of the simplex in relation to the $n+1$ point. If the objective function of the new

model obtained was smaller than the highest value of the initial population, the model was replaced.

The search domain was limited to the same ranges used in the above sensitivity tests of the dispersion curves and in the objective function maps. The stopping criteria of the algorithm was the maximum number of 10000 iterations or the minimum value of 0.01% of the objective function.

Figure 8 shows scatterplots of the seismic parameters of the population of models obtained at each iteration during the run of the inversion algorithm. These plots record the trajectory of the model population around the synthetic reference model for each iteration. In this way, we can evaluate the convergence process of the inversion algorithm in terms of accuracy (if the parameters converge to the correct values), efficiency (convergence speed), and uncertainty of the estimates of each of the parameters

(standard deviation of the distribution of values of the final population of the models).

The algorithm reaches the stopping criterion with less than 5000 iterations. Vs_1 and Vs_3 are the fastest convergence parameters (about 1000 iterations) followed by h_1 (3000 iterations), and best determined from the model, as previously established by the objective function analysis. Vs_2 and h_2 tend to converge after 5000 iterations with the population of models oscillating around the real value, indicating the presence of uncertainty in the estimation of the parameters, while densities and Vp_2 are the most difficult parameter to fit the model. Vp_1 and Vp_3 slowly converge to the correct values due to the low sensitivity of these parameters in the dispersion curves. Furthermore, the parameters corresponding to layer 2 are more poorly fitted when compared to the other layers.

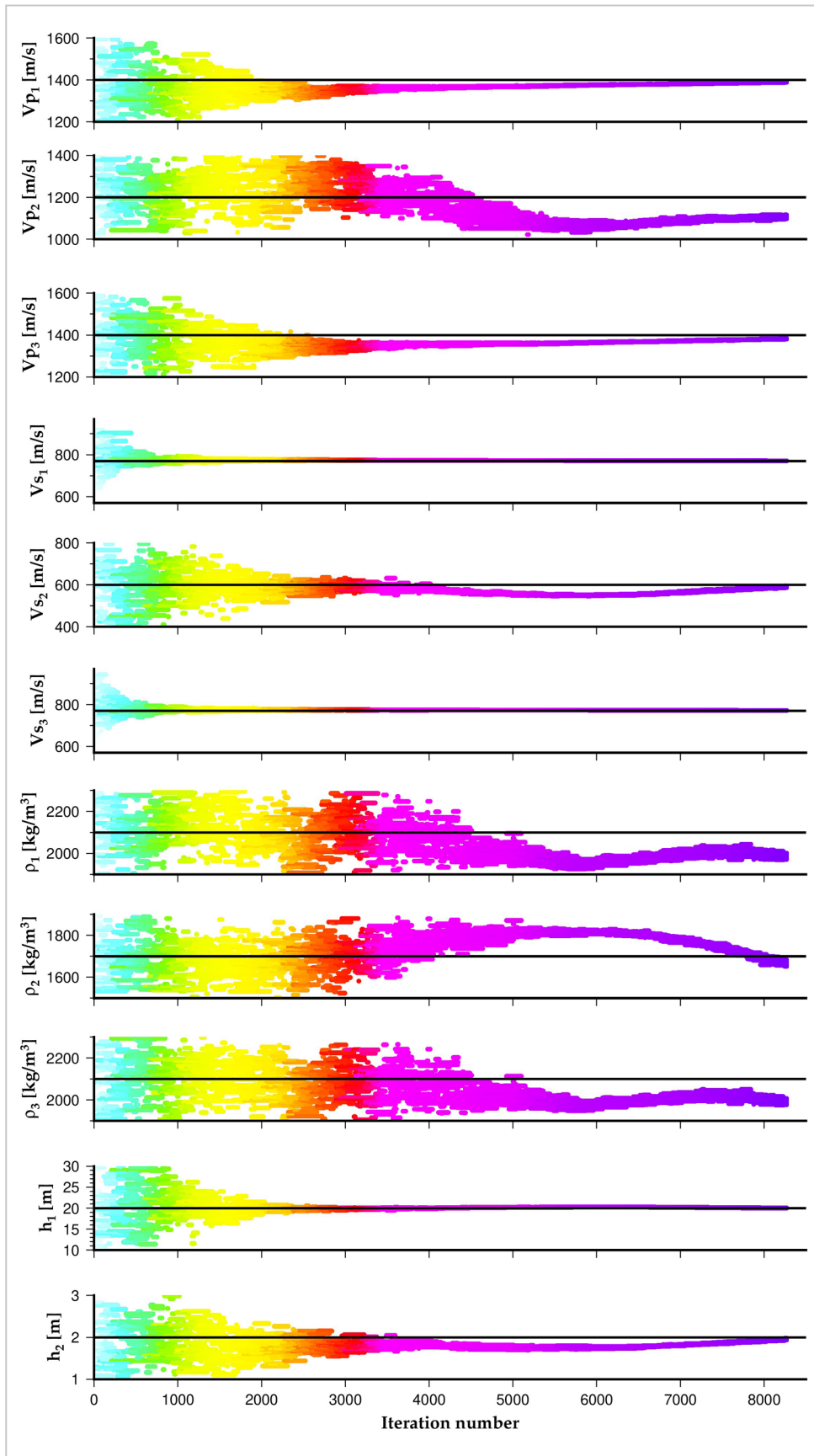


Figure 8 - Scatter plots of the parameters V_p , V_s , density and thickness of each layer of the population of models (vertical axis) in terms of the iteration number of the inversion algorithm (horizontal axis). The solid black line is the reference line on the true value of the parameter. The colors of the dots are related to the misfit value of the related model.

Figure 9 shows the misfit between the dispersion curves corresponding to the synthetic reference model and

the best model (lowest misfit value) obtained after 8268 iterations of the inversion algorithm. The parameters of

the synthetic model and the best model obtained from inversion are presented in Table 2.

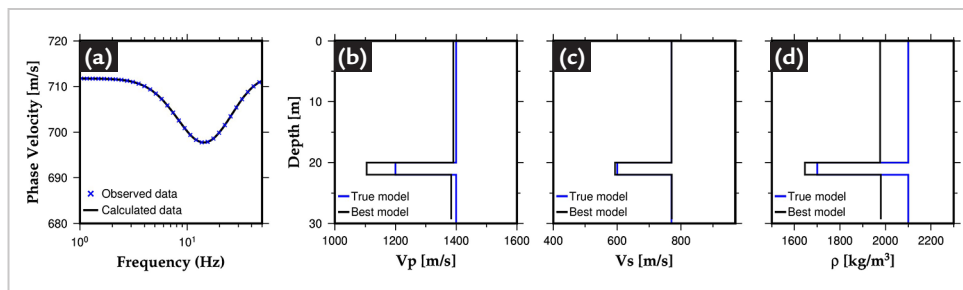


Figure 9 - (a) Misfit of the dispersion curves corresponding to the synthetic reference model (blue crosses) and the best model (black line). (b) V_p , (c) V_s and (d) density profiles resulting from the best model (black lines) in relation to the profiles of the target synthetic model (blue line).

Table 2 - Comparison of parameter values of the synthetic model and the best model obtained from the implemented CRS algorithm.

Parameter	True Value	Best Model	Error (%)
V_{p_1}	1400 m/s	1403.30 m/s	0.23
V_{p_2}	1200 m/s	1323.93 m/s	10.32
V_{p_3}	1400 m/s	1413.03 m/s	0.9
V_{s_1}	770 m/s	769.78 m/s	0.03
V_{s_2}	600 m/s	561.37 m/s	6.4
V_{s_3}	770 m/s	769.19 m/s	0.11
ρ_1	2100 kg/m ³	2039.42 kg/m ³	2.88
ρ_2	1700 kg/m ³	1648.56 kg/m ³	3.02
ρ_3	2100 kg/m ³	2060.43 kg/m ³	1.88
h_1	20 m	20.28 m	1.4
h_2	2 m	1.61 m	19.5

8. Summary and conclusions

This study aimed to investigate the applicability of the MASW seismic method in coal prospecting at the Candiotá mine, southern Brazil. Theoretical tests were carried out with synthetic data generated from models designed from drilling and well cores.

In general, sensitivity tests of the seismic model parameters indicated the variations in the values of V_p and density of the three layers of the model do not cause significant changes in the dispersion curves obtained. The V_s parameter was the main responsible for the changes in the dispersion curves.

Therefore, the study demonstrated that the seismic model parameters inferred from the surface wave dispersion curves data allow a proper solution to be determined for the layer structure in terms of S wave velocity, as well as layer thicknesses.

The analysis of objective function maps supported the sensitivity tests from the visualization of the non-uniqueness and resolution of the parameters involved in the inversion problem.

The implemented CRS inversion algorithm proved to be able to recover accurately a model represented by seis-

mic velocity inversion and thin layer, which according to the local geological setting may be associated with the presence of a coal seam.

In short, the study demonstrated that the MASW method has great potential in the exploration of mineral resources associated with the carboniferous systems present in southern Brazil. Future studies should advance in the application of the inversion algorithm with real seismic data acquired in the study region and correlation with the geological information of the drillholes.

References

- BENTES, M.; COSTA, A. F. U. Prospecção geofísica para carvão. Rio de Janeiro, CPRM, 1979. Available in: <https://rigeo.sgb.gov.br/handle/doc/13796>
- BORTOLOZO, C. A.; PORSANI, J. L.; DOS SANTOS, F. A. M.; ALMEIRA, E. R. VES/TEM 1D joint inversion by using Controlled Random Search (CRS) algorithm. *Journal of Applied Geophysics*, 112, p. 157-174, 2015.
- BUCHANAN, D. J.; DAVIS, R.; JACKSON, P. J.; TAYLOR, P. M. Fault location by channel wave seismology in United Kingdom coal seams. *Geophysics*, v. 46, n. 7, p. 994-1002, 1981.
- CAGLIARI, J.; LAVINA, E. L. C.; PHILIPP, R. P.; TOGNOLI, F. M. W.; BASEI, M. A. S.; FACCINI, U. F. New Sakmarian ages for the Rio Bonito formation (Paraná Basin, southern Brazil) based on LA-ICP-MS U-Pb radiometric dating of zircons crystals. *Journal of South American Earth Sciences*, 56, p. 265-277, 2014.

- CHARILOGIS, V.; TSOULOS, I.; TZALLAS, A.; ANASTASOPOULOS, N. An improved controlled Random Search Method. *Symmetry*, v. 13, n. 11, 1981, 2021.
- CHRISTOFFEL, D. A.; KAYAL, J. R. Coal quality from geophysical logs: Southland lignite region, New Zealand. *The Log Analyst*, v. 30, n. 05, 1989.
- COSTA, A. F. U.; PUTY, C. O. F. D.; FERREIRA, J. A. F.; BENTES, M.; DIAS, N. L. Projeto Geofísica Terrestre para carvão em Santa Catarina e Rio Grande do Sul. *Technical Report*, Porto Alegre: CPRM, 1978. Available in: <https://rigeo.sgb.gov.br/handle/doc/7917>
- COSTA, A. F. U.; DIAS, N. L. Geofísica aplicada à prospecção de carvão na área do Bloco 1, Rio Pardo, RS, *Acta Geológica Leopoldensia*, 6, p. 5-13, 1982.
- DI MAIO, R.; RANI, P.; PIEGARI, E.; MILANO, L. Self-potential data inversion through a genetic-price algorithm. *Computers & geosciences*, 94, p. 86-95, 2016.
- DRESDEN, L.; RUTER, H. Seismic coal exploration. Part B: in-seam seismics. *International Journal of Rock Mechanics and Mining Sciences and Geomechanics Abstracts*, v. 1, n. 33, p. 25A, 1996.
- FOTI, S.; HOLLENDER, F.; GAROFALO, F.; ALBARELLO, D.; ASTEN, M.; BARD, P. Y.; SOCCO, V. Guidelines for the good practice of surface wave analysis: a product of the InterPACIFIC project. *Bulletin of Earthquake Engineering*, 16, p. 2367-2420, 2018.
- GOCHIOCO, L. M. Seismic surveys for coal exploration and mine planning. *The Leading Edge*, v. 9, n. 4, p. 25-28, 1990.
- GOCHIOCO, L. M. High-resolution 3-D seismic survey over a coal mine reserve area in the US - a case study. *Geophysics*, v. 65, n. 3, p. 712-718, 2000.
- GOCHIOCO, L. M.; COTTEN, S. A. Locating faults in underground coal mines using high-resolution seismic reflection techniques. *Geophysics*, v. 54, n. 12, p. 1521-1527, 1989.
- GOMES, A. P.; FERREIRA, J. A. F.; ALBUQUERQUE, L. F. D.; SÜFFERT, T. Carvão fóssil. *Estudos Avançados*, 12, p. 89-106, 1998.
- GREENHALGH, S. A.; SUPRAJITNO, M.; KING, D. W. Shallow seismic reflection investigations of coal in the Sydney Basin. *Geophysics*, v. 51, n. 7, p. 1426-1437, 1986.
- HATHERLY, P. Overview on the application of geophysics in coal mining. *International Journal of Coal Geology*, 114, 74-84, 2013.
- HOLZ, M.; VIEIRA, P. E.; KALKREUTH, W. The Early Permian coal-bearing succession of the Paraná Basin in southernmost Brazil: depositional model and sequence stratigraphy. *Revista Brasileira de Geociências*, v. 30, n. 3, p. 420-422, 2000.
- HOLZ, M.; KALKREUTH, W. Sequence stratigraphy and coal petrology applied to the Early Permian coal-bearing Rio Bonito Formation, Paraná Basin, Brazil. In: PASHIN, J. C. ; GASTALDO, R. A. (ed.). Sequence stratigraphy, paleoclimate, and tectonics of coal-bearing strata: *AAPG Studies in Geology*, v. 51, p. 147-167, 2004.
- KAELO, P.; ALI, M. M. Some variants of the controlled random search algorithm for global optimization. *Journal of Optimization Theory and Applications*, 130, p. 253-264, 2006.
- KRIVÝ, I.; TVRDÍK, J. The controlled random search algorithm in optimizing regression models. *Computational Statistics & Data Analysis*, v. 20, n. 2, p. 229-234, 1995.
- KOKOWSKI, J.; SZREDER, Z.; PILECKA, E. Reference P-wave velocity in coal seams at great depths in Jastrzebie coal mine. In: E3S WEB OF CONFERENCES, v. 133, p. 01011, 2019. (EDP Sciences).
- KREY, T. C. Channel waves as a tool of applied geophysics in coal mining. *Geophysics*, v. 28, n. 5, p. 701-714, 1963.
- LOWRIE, W. *Fundamentals of geophysics*. New York: Cambridge University Press, 2007. 381 p.
- MACHADO, E. R.; CASTANHO, O. S. Pesquisa de carvão mineral na faixa sedimentar do Rio Grande do Sul. *Publication of Departamento Autônomo de Carvão Mineral*, 42, 1956.
- MORCOTE, A.; MAVKO, G.; PRASAD, M. Dynamic elastic properties of coal. *Geophysics*, v. 75, n. 6, E227-E234, 2010.
- OLSSON, D. M.; NELSON, L. S. The Nelder-Mead simplex procedure for function minimization. *Technometrics*, v. 17, n. 1, p. 45-51, 1975.
- PARK, C. B.; MILLER, R. D.; XIA, J. Multichannel analysis of surface waves. *Geophysics*, v. 64, n. 3, p. 800-808, 1999.
- PARK, C. B.; MILLER, R. D.; XIA, J.; IVANOV, J. Multichannel analysis of surface waves (MASW) - active and passive methods. *The Leading Edge*, v. 26, n. 1, p. 60-64, 2007.
- PRICE, W. L. A controlled random search procedure for global optimisation. *The Computer Journal*, v. 20, n. 4, p. 367-370, 1977.
- SHERIFF, R. E.; GELDART, L. P. *Exploration seismology*. Cambridge university press, 1995.
- SILVA, J. B.; HOHMANN, G. W. Nonlinear magnetic inversion using a random search method. *Geophysics*, v. 48, n. 12, p. 1645-1658, 1983.
- SILVA, Z. C. Candiota coalfield: a world class Brazilian coal deposit. *International Journal of Coal Geology*, v. 23, n. 1-4, p. 103-116, 1993.
- SILVA, M. B.; KALKREUTH, W. Petrological and geochemical characterization of Candiota coal seams, Brazil - implication for coal facies interpretations and coal rank. *International Journal of Coal Geology*, v. 64, n. 3-4, p. 217-238, 2005.
- SMITH, D. N.; FERGUSON, J. F. Constrained inversion of seismic refraction data using the controlled random search. *Geophysics*, v. 65, n. 5, p. 1622-1630, 2000.

- SOUZA, V. D.; SALVADORETTI, P.; COSTA, J. F. C. L.; BERETTA, F.; KOPPE, J. C.; BASTIANI, G. A.; GRIGORIEFF, A. Estimativa de qualidade de carvão por meio de perfilagem geofísica de gama natural e resistividade. *REM - Revista Escola de Minas*, v. 63, p. 653-660, 2010.
- THOMAS, L. P. Global standardization of coal resources and reserves. *In: The Coal Handbook*: Woodhead Publishing, 2023. p. 53-83.
- TIAN, M.; HAN, L.; MENG, Q.; JIN, Y.; MENG, L. In situ investigation of the excavation-loose zone in surrounding rocks from mining complex coal seams. *Journal of Applied Geophysics*, 168, p. 90-100, 2019.
- ZALAN, P. V.; WOLFF, S.; CONCEIÇÃO, J. C. J.; MARQUES, A. ASTOLFI, M. A. M.; VIEIRA, I. S.; APPI, V. T.; ZANOTTO, O. A. Bacia do Paraná. *In: RAJA-GABAGLIA, G. P. ; MILANI, E. J. (org.). Origem e evolução de bacias sedimentares*. Rio de Janeiro: Petrobras, 1990.
- WATHELET, M.; CHATELAIN, J. L.; CORNOU, C.; GIULIO, G. D.; GUILLIER, B.; OHRNBERGER, M.; SAVVAIDIS, A. Geopsy: a user friendly open source tool set for ambient vibration processing. *Seismological Research Letters*, v. 91, n. 3, p. 1878-1889, 2020.
- WEBBER, T.; SALVADORETTI, P.; KOPPE, J. C.; COSTA, J. F. C. L. Estimativa de parâmetros indicadores de qualidade de carvão a partir de perfilagem geofísica. *REM - Revista Escola de Minas*, 62, p. 283-289, 2009.
- WORLD COAL INSTITUTE - WCI. *Coal & Steel*. London: WCI report, 2009.

Received: 12 December 2023 - Accepted: 12 March 2024.